Solid State Science and Technology, Vol. 19, No2 (2011) 221-231
ISSN 0128-7389

SYNTHESIS AND CHARACTERIZATION OF $Bi_3Mg_2Nb_3O_{14}$ PYROCHLORE SYSTEM

P.Y. Tan[1], K.B. Tan[1,*], C. C. Khaw[3], Z. Zainal[1] and S.K. Chen[2]

[1]*Department of Chemistry, Faculty of Science, Universiti Putra Malaysia, 43400 Serdang, Selangor*

[2]*Department of Physic, Faculty of Science, Universiti Putra Malaysia, 43400 Serdang, Selangor*

[3] *Faculty of Engineering and Science, University Tunku Abdul Rahman, 53300 Kuala Lumpur, Malaysia*

**Corresponding author: tankb@science.upm.edu.my*

ABSTRACT

Synthesis of $Bi_3Mg_2Nb_3O_{14}$ pyrochlore was carried out using conventional solid-state method. Phase formation and electrical properties of $Bi_3Mg_2Nb_3O_{14}$ pyrochlore was investigated by employment of different spectroscopy techniques. The phase purity and formation mechanism were confirmed by X-ray diffraction analysis. The "ideal" $Bi_3Mg_2Nb_3O_{14}$ was formed at 1025 °C as cubic pyrochlore with minute traces of $Mg_4Nb_2O_9$ and $MgNb_2O_6$ phases. The determined grain size by SEM analysis was found in the range of 1.5 - 6.5 μm. Impedance spectroscopy study revealed that $Bi_3Mg_2Nb_3O_{14}$ pyrochlore was highly resistive with high activation energy of 1.36 eV. The recorded dielectric constant, ε', was ~110; dielectric loss, tan δ, 10^{-3}, both at room temperature and at frequency 1 MHz. No sign of ionic conduction was discerned and the mechanism was probably attributed to hopping-type.

Keywords: phase formation; sintering; pyrochlore; solid state;

INTRODUCTION

The structure of pyrochlore has a general formula of $A_2B_2O_6O'$ with four crystallographically nonequivalent kinds of atoms in which A and B are metal ions, e.g. $(Bi_{1.5}Zn_{0.5})(Zn_{0.5}Nb_{1.5}O)_7$ (α-BZN) and $(Bi_{1.5}Zn_{0.5})(Zn_{0.5}Ta_{1.5}O_7)$ (α-BZT). It is also known that pyrochlore structure is a derivative of fluorite structure. The A cations are eight coordinated that contain six equal A-O and two equal A-O' distances and are located within distorted cubes. The smaller B cations are coordinated with six equal B-O distances and located within trigonal antiprisms. Oxides with the pyrochlore structure provide a host lattice suitable for incorporation of aliovalent dopants, interstitial oxygen, protons, and electronic defects [1-2].

The advancement in the production technology of electronic ceramic has led on to

enormous miniaturization of electronic components. Highly dielectric ceramics make it possible to markedly miniaturize passive microwave components. These ceramics must have the requirement of high permittivity and extremely low tan δ losses. Pyrochlore oxides with the formula $(Bi_{1.5}Zn_{0.5})(Zn_{0.5}Nb_{1.5}O)_7$ (α-BZN) and $(Bi_{1.5}Zn_{0.5})(Zn_{0.5}Ta_{1.5}O_7)$ (α-BZT) have emerged as good low sintering microwave materials which have the potential as capacitor and high-frequency filter applications due to their excellent dielectric constant and low dielectric loss, tan δ, 10^{-3}-10^{-4} [3-7].

Two different compositions with cubic pyrochlore and monoclinic zirconolite phases in the Bi_2O_3-ZnO-Nb_2O_5 system have been identified as potential low-fired dielectric composites for high-frequency multilayer devices [8-11]. MgO is well known as low dielectric loss and its comparable ionic radius, 0.72 Å to ZnO, 0.74 Å; hence, it has been chosen to replace ZnO in the preparation of pyrochlore materials. The present paper discusses the results of phase formation and electrical properties of $Bi_3Mg_2Nb_3O_{14}$ pyrochlore.

EXPERIMENTAL DETAILS

$Bi_3Mg_2Nb_3O_{14}$ pyrochlore was prepared by conventional solid state method. The starting materials were reagent grade oxide powders, Bi_2O_3 (Alfa Aesar, 99.99%), MgO (Aldrich, 99%) and Nb_2O_5 (Alfa Aesar, 99.9%) All oxide powders were pre-fired at different temperatures in which Bi_2O_3 was at 300 °C and the others at 600 °C for 3 hours, respectively. Stoichiometric amounts of oxides were weighed and mixed homogeneously with acetone in agate mortar. The resulted mixed powder was then transferred into platinum boat and heated at 300 °C for 1 hour, 600 °C for 1 hour and 800 °C for 24 hours. The firing temperatures were increased gradually from over 800 °C to 1100 °C with heating duration of 24 hours for every incremental step of 25 °C. Intermediate regrinding was employed to refresh the contact area of the reactants. There was no significant weight loss within the firing temperature ranging from 800 °C to 1050 °C. Approximately 1% weight loss was recorded between 1075 °C and 1100 °C. The powders were pressed into pellets of 8 mm in diameter and ~ 1.5 mm in thickness prior to sintering at 1025 °C for 24 hours.

Densities of the pellets (experimental densities) were calculated using the following formula:

$$Density,\ D = \frac{mass}{volume} \qquad (1)$$

On the other hand, the theoretical density of the sample was calculated with the following formula:

$$D = \frac{FW \times Z}{V \times N} \qquad (2)$$

where FW is the formula weight, *N* is Avogadro's number, *Z* is formula units and V is

volume of one formula unit x *Z*. The relative densities of the prepared samples were compared between experimental and theoretical densities.

The phase purities of prepared sample were examined by X-ray powder diffraction using an automated Shimadzu diffractometer XRD 6000, Cu Kα radiation in 2θ range of 10-70° at the scan speed of 2°/min. Surface morphologies of $Bi_3Mg_2Nb_3O_{14}$ pyrochlore annealed at 1025°C were analyzed using scanning electron microscopy (SEM).

The electrical properties of the samples were investigated by HP4192A AC impedance analyzer in the frequency range of 5 Hz to 13 MHz. Electrical measurements were performed in temperature ranging from 25 to 800 °C. The gold electrodes were deposited on the both faces of the pellets by a gold paste and then hardened from 200 °C to 600 °C.

RESULTS AND DISCUSSION

X-ray and SEM analyses

Figure 1 shows the X-ray diffraction (XRD) patterns of $Bi_3Mg_2Nb_3O_{14}$ heated at different temperatures in the temperature range of 800 °C to 1100 °C. Below temperature 875 °C, cubic pyrochlore, $BiNbO_4$ and $Bi_5Nb_3O_{14}$ phase are observed.

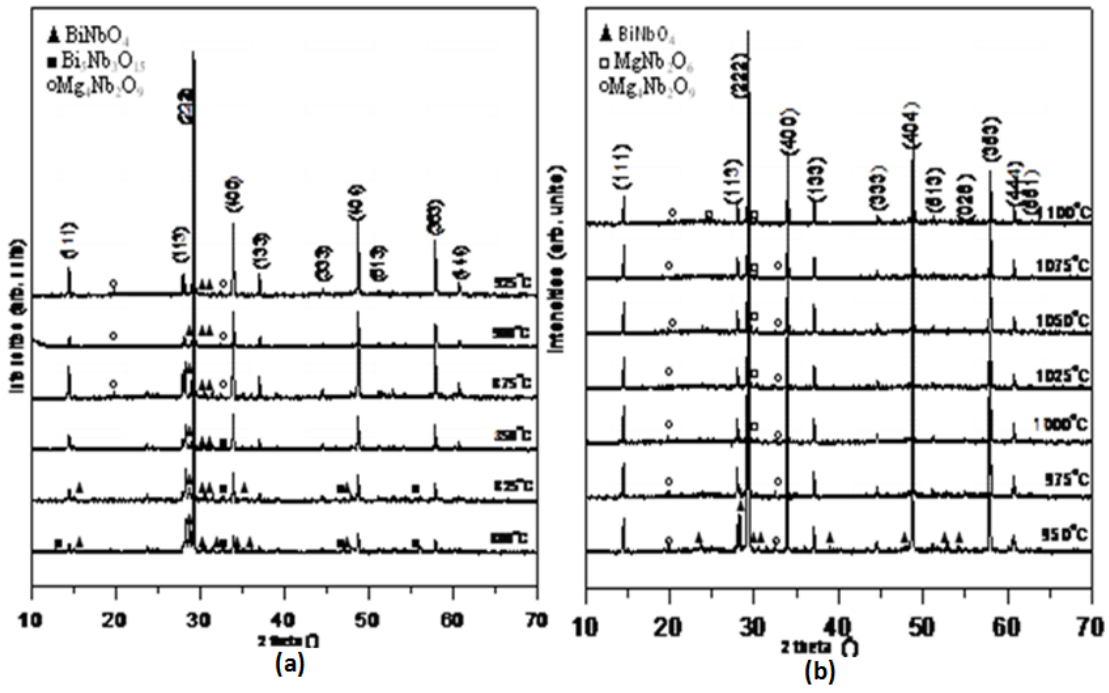

Figure 1: X-ray diffraction patterns for the $Bi_3Mg_2Nb_3O_{14}$ annealed at (a) 800 °C to 925 °C and (b) 950 °C to 1100 °C

Between temperature 875 °C to 1000 °C, it is clear that the sample is a mixed phase in which cubic pyrochlore, $BiNbO_4$ and $Mg_4Nb_2O_9$ are coexisted. When the sample is heated above 1000 °C, $BiNbO_4$ phase diminishes but intensity of $Mg_4Nb_2O_9$ phase increases. Meanwhile, other secondary phase, $MgNb_2O_6$ is formed and the intensity is found notably increases with temperature. At the final sintering temperature, 1100 °C, cubic pyrochlore, $Mg_4Nb_2O_9$ and $MgNb_2O_6$ phases are discernable. However, the intensity of overall peaks is reduced and there is a significant weight loss, i.e. more than 1% of weight loss.

The reaction mechanisms of the formation of $Bi_3Mg_2Nb_3O_{14}$ pyrochlore are proposed as below:

At 800 °C < T < 875 °C,
$5\ Bi_2O_3 + 4\ Nb_2O_5 + 2\ MgO \rightarrow\ Bi_3Mg_2Nb_3O_{14} + 2\ BiNbO_4 + Bi_5Nb_3O_{15}$

At 875 °C < T < 1000 °C,
$BiNbO_4 + Bi_5Nb_3O_{15} + 6\ MgO + 2\ Nb_2O_5 \rightarrow Bi_3Mg_2Nb_3O_{14} + 3\ BiNbO_4 + Mg_4Nb_2O_9$

At 1000 °C < T <1100 °C,
$2\ Mg_4Nb_2O_9 + 3\ BiNbO_4 + Nb_2O_5 \rightarrow Bi_3Mg_2Nb_3O_{14} + Mg_4Nb_2O_9 + 2\ MgNb_2O_6$

In conclusion, the starting oxides are reacted at temperature below 875 °C to form mixed pyrochlore phase. However, $BiNbO_4$ and $Bi_5Nb_3O_{15}$ are not stable at higher temperature and decomposed after reaction with Nb_2O_5 and MgO. It is also difficult to eliminate $MgNb_2O_6$ phase. The phase formation of $Bi_3Mg_2Nb_3O_{14}$ pyrochlore can be summarized in Table 1.

Table 1: Phase formation of $Bi_3Mg_2Nb_3O_{14}$ sample at different temperatures

Temperature(°C)	800 < T < 875	875 < T < 1000	1000 < T < 1100
Phases formed in the sample	Cubic pyrochlore + $BiNbO_4$ + $Bi_5Nb_3O_{15}$	Cubic pyrochlore + $BiNbO_4$ + $Mg_4Nb_2O_9$	Cubic pyrochlore + $Mg_4Nb_2O_9$ + $MgNb_2O_6$

Surface micrographs of $Bi_3Mg_2Nb_3O_{14}$ pyrochlore are shown in Figure 2. Different magnifications, e.g. 1000 X and 5000 X are used in order to gain further insight into the microstructure of pyrochlore. The SEM analysis reveals that the grain size of the sample is in the range of 1.5 - 6.5 μm. The relative density of the sample is calculated using the formula in (1) and (2). The sample appears to be porous which agrees reasonably with the relative density of 82%.

Solid State Science and Technology, Vol. 19, No2 (2011) 221-231
ISSN 0128-7389

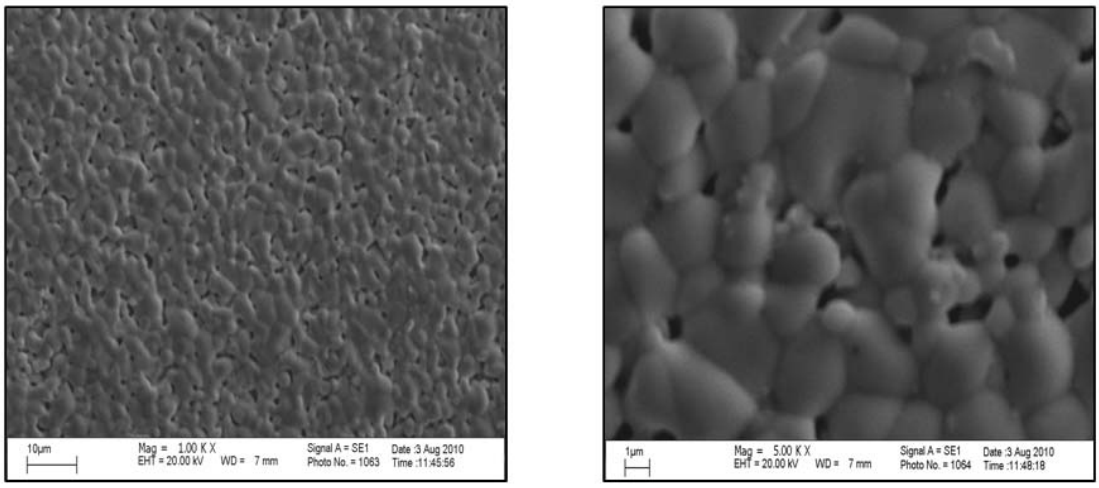

(a) (b)

Figure 2: SEM micrographs of $Bi_3Mg_2Nb_3O_{14}$ (a) Mag. = 1.00 K (b) Mag. = 5.00 K sintered at 1025°C for 24 hours

Electrical properties

Cole-cole plots of the $Bi_3Mg_2Nb_3O_{14}$ sintered at 1025 °C at different temperatures are shown in Figure 3 (a) and (b). The impedance data are normalized by the geometric factor. The electric conductivity response of pyrochlore is studied in time domain, e.g. τ = RC. Perfect semicircles are observed for all the measurements at temperature range 550-800 °C and the capacitance values at all the temperatures are in the order of 10^{-12} F cm^{-1}, which are typical of bulk materials. This sample has the capacitance of 7.62 x 10^{-12} F cm^{-1} at 600 °C. No grain boundary effect is observed from the cole-cole plots. There is no sign of spike arising from ionic conduction at the low frequency region. Thus, the response should be associated with the electronic conducting type. The electrical data are well represented by parallel RC circuit of the bulk material; R_b and C_b are bulk resistance and capacitance, respectively [7, 13]. Combined spectroscopic plots, Figure 4 shows two coincident peaks of imaginary part of complex modulus, *M"* and imaginary part of complex impedance, *Z"* indicating that no grain boundary effect. The material is homogenous with the evidence of the full width at half maximum (FWHM) of the *M''* peak is approximately 1.20 decades which is closed to the perfect Debye (1.14 decade).

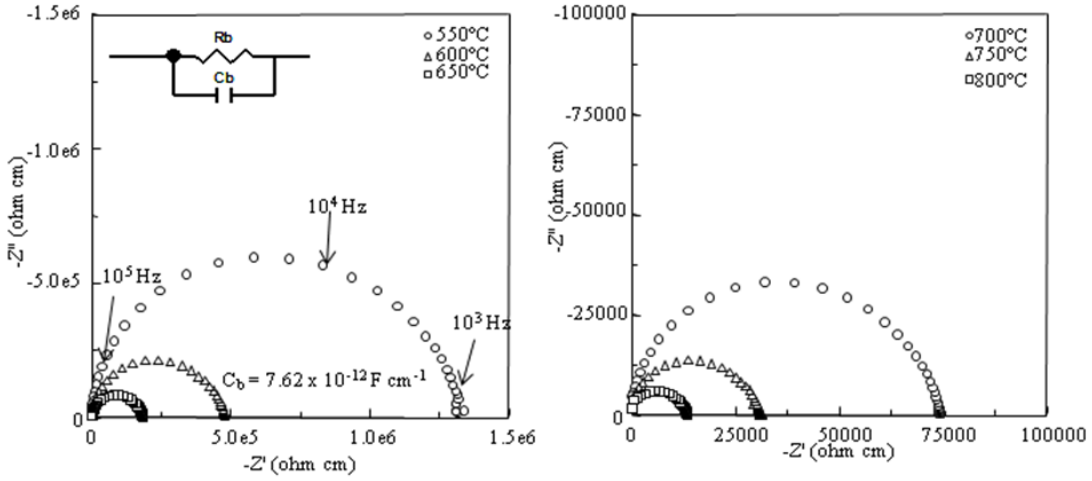

Figure 3: Complex plots of $Bi_3Mg_2Nb_3O_{14}$ at different temperatures

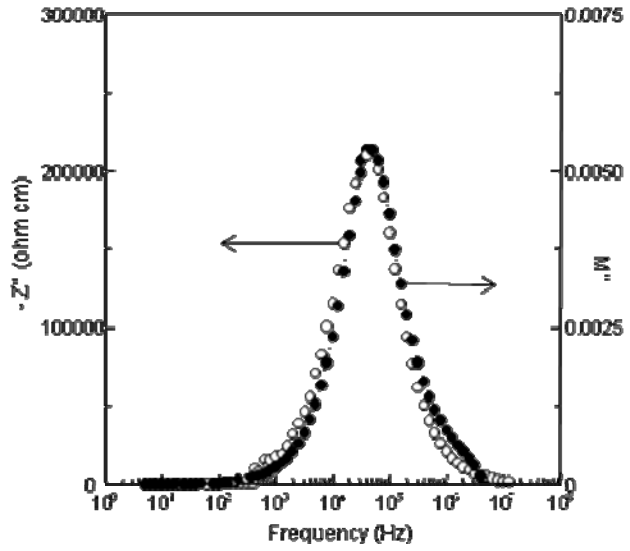

Figure 4: Combined spectroscopic plots of $Bi_3Mg_2Nb_3O_{14}$ at 650 °C

Figure 5 shows the temperature variation of total conductivity in $Bi_3Mg_2Nb_3O_{14}$ sample via conductivity Arrhenius plots. Conductivity values are extracted from cole-cole plot. The data are reversible on heat and cool cycles. A linear behaviour is discernable with activation energy of 1.36 eV on heating cycle. There is negligible change in activation energy, i.e. 1.30 eV when cooled down from 800 °C to 500 °C. The activation energy is lower than that of BZN (~1.59 eV) and BZT (1.55 eV) but is similar to BZS (1.37 eV). Typically, high activation energy when not linked to the ionic conductivity usually related to a hopping type electronic mechanism, which suggests the presence of defect of the oxygen vacancy type [7, 13].

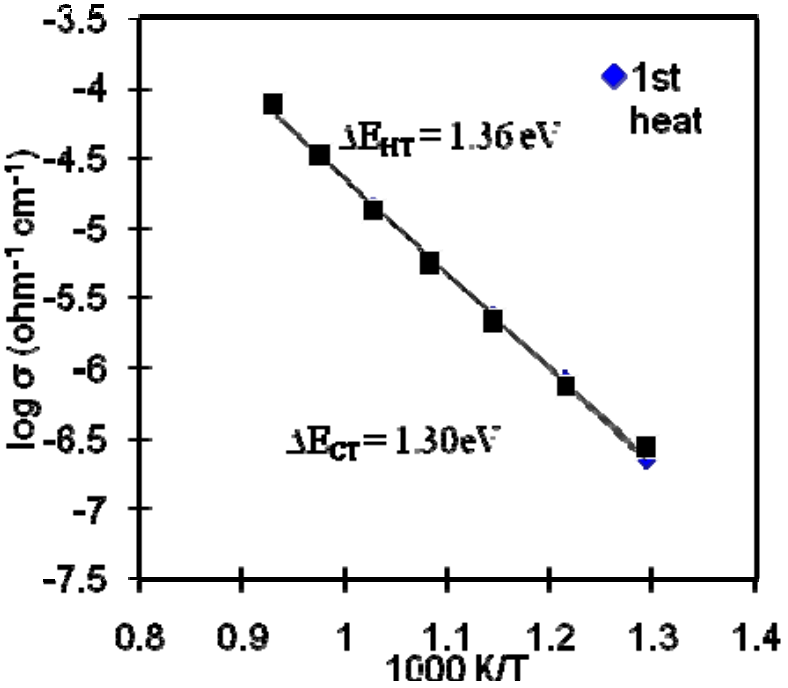

Figure 5: Conductivity Arrhenius plots of $Bi_3Mg_2Nb_3O_{14}$ sintered at 1025 °C

Dielectric response as a function of temperature for $Bi_3Mg_2Nb_3O_{14}$ was studied in the frequency range of 5 Hz - 13 MHz. Only frequencies at 1 kHz, 100 kHz and 1 MHz are selected for the study of the dielectric response of the sample at different temperatures (Figure 6 and Figure 7). The apparent rise in both dielectric constant, ε' and dielectric loss are observed above 500 °C onwards for every frequency. As the temperature increased, ε' and tan δ increase due to higher degree of polarization. The changes of ε' and tan δ with frequencies in pyrochlore could possibly attributed to the hopping conduction mechanism [1, 7, 12-13]. The increases in ε' with temperature gives this material a negative temperature coefficient. The temperature coefficient of relative permittivity, TCε', is calculated using the following formula:

$$TC\varepsilon' = \varepsilon'_{T2} - \varepsilon'_{T1} / \varepsilon'_{T1} (T_2 - T_1) \qquad (4)$$

where ε'_{T1} is the relative permittivity measured at T_1, 25 °C and ε'_{T2} is the relative permittivity measured at T_2, 300 °C. TCε' for this sample is ~ -480 ppm/°C measured at 1MHz. This value is comparable to the reported value in cubic BZN pyrochlore, TCε' ~ -500 ppm/°C.

Mixed phase $Bi_3Mg_2Nb_3O_{14}$ shows high ε' value, ~110 and tan δ, 10^{-3} at 25 °C at 1 MHz. The dielectric constant of this sample is comparable to BZN analogue which exhibits dielectric constant of 80 - 150. On the other hand, the value of dielectric constant of $Bi_3Mg_2Nb_3O_{14}$ is much higher than that of BZT (~58 – 71) and

$Bi_3Zn_2Sb_3O_{14}$ (BZS) (~32).

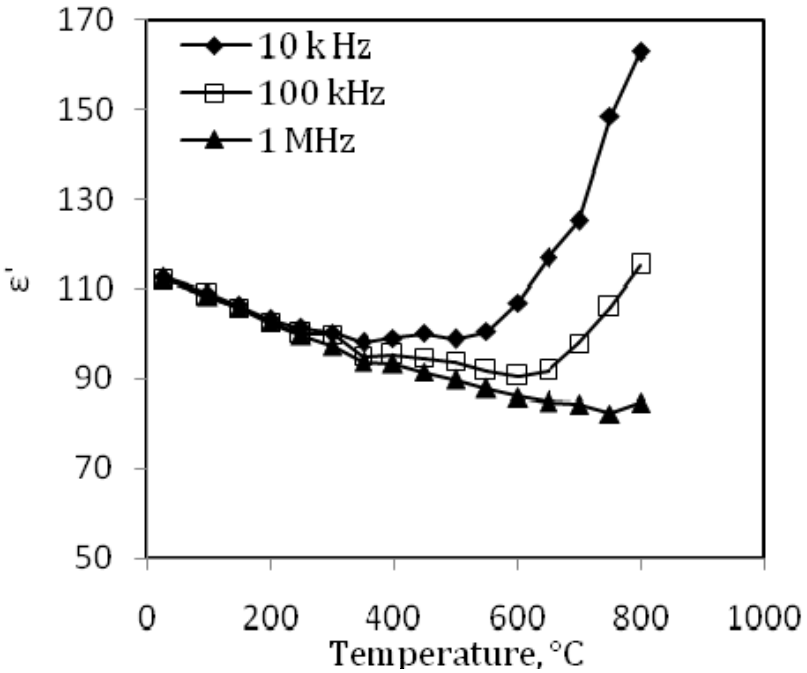

Figure 6: Dielectric constant, ε' of $Bi_3Mg_2Nb_3O_{14}$ as a function of temperatures at different frequencies

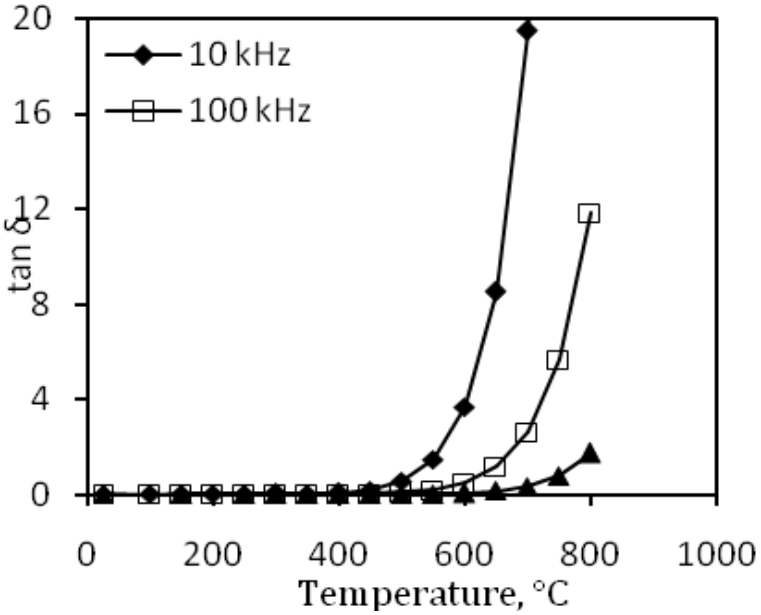

Figure 7: Dielectric loss, tan δ of $Bi_3Mg_2Nb_3O_{14}$ as a function of temperatures at different frequencies

Figure 8 and Figure 9 show the ε' and tan δ as a function of frequencies. Both ε' and tan δ decrease with increasing frequency could be explained by the lower degree of polarization. As the frequency increases, the jumping frequency of electric charge carriers cannot follow the alternation of applied AC electric field due to the time constraint. A high degree of dispersion of dielectric constant of $Bi_3Mg_2Nb_3O_{14}$ at low frequencies (<1 kHz) is observed. In the frequency range below 1 kHz, non- frequency dependent response is observed for temperature range below 500 °C (Figure 6). This dispersion may be attributed to the confined polarization. The space charge polarization is governed by the number of space charge carriers. These behaviours are similar to $Bi_{1.5}ZnTa_{1.5}O_7$ and $Bi_3Zn_2Sb_3O_{14}$ dielectric ceramics, in which a conduction mechanism of the hopping type involved.

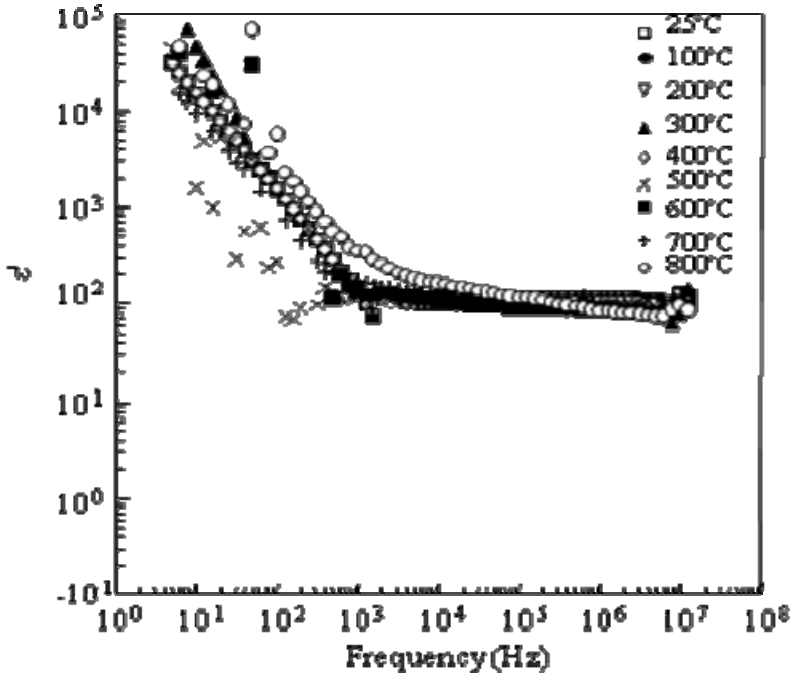

Figure 8: Dielectric constant, ε' of $Bi_3Mg_2Nb_3O_{14}$ as a function of frequency at different temperatures

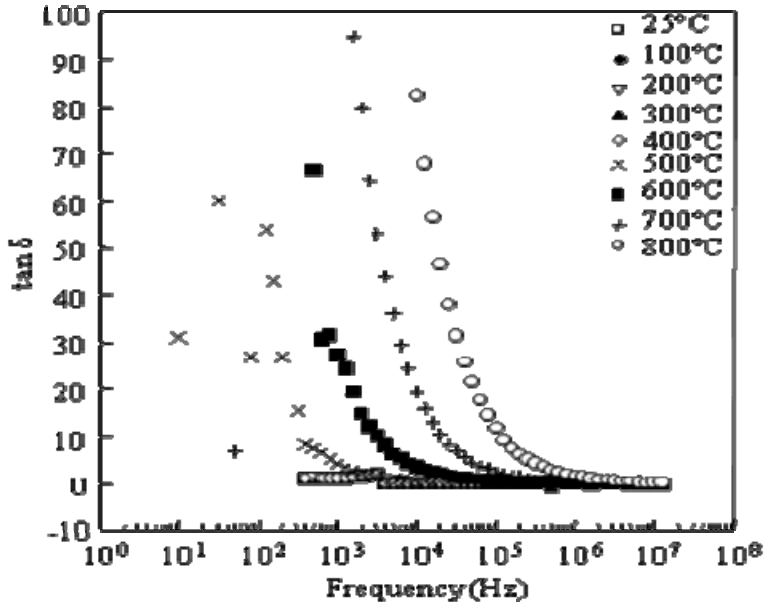

Figure 9: Dielectric loss, tan δ of $Bi_3Mg_2Nb_3O_{14}$ as a function of frequency at different temperatures

CONCLUSION

The phase formation of $Bi_3Mg_2Nb_3O_{14}$ pyrochlore sample was carefully studied. The sample existed as mixed phase after heat treatment at temperature 1025 °C. $Bi_3Mg_2Nb_3O_{14}$ pyrochlore showed dielectric constant, ε'~110 and tanδ~10^{-3} at 1 MHz at ambient temperature. There was no indication of ionic conductivity in which a hoping conduction mechanism was proposed. The temperature coefficient of relative permittivity, TCε' for this sample was ~ -480 ppm/°C at 1 MHz.

ACKNOLEDGEMENT

Financial support from Ministry of Higher Education, Malaysia via Fundamental Research Grant Scheme (FRGS) (5523620) is gratefully appreciated.

REFERENCES

[1] Du H, Wang H, Yao X. Ceram. Int. , **30** (7) (2004) 1383-1387
[2] Subramanian M., Aravamudan G., Rao G.V.S. Prog. Solid St.Chem., **15** (1985) 55-143
[3] Wersing W. High-frequency ceramic dielectrics and their application for microwave components. In Electronic Ceramics. Steele, B.C.H. Ed. (England: Elsevier Science Publisher LTD, 1991) 67-119
[4] Du H, Yao X, Zhang X, Weng H. Appl. Surf. Sci., **253** (4) (2006) 1856-1860

[5] Wu M.C., Kamba S, Bovtun V, Su W.F. J. Eur. Ceram. Soc., **26** (10-11) (2006) 1889-1893
[6] Zanetti S, Pereira M, Nono M. J. Eur. Ceram. Soc. **27** (13-15) (2007) 3647-3650
[7] Khaw C.C., Tan K.B., Lee C.K. Ceram. Int. **35** (2009) 1473-1480
[8] Nino J.C., Lanagan M.T., Randall C.A. J. Mater. Res. **16** (5) (2001) 1460
[9] Tan K.B., Lee C.K., Zainal Z, Khaw C.C., Tan Y.P., Shaari H. (2008). Reaction Study and Phase Formation in Bi_2O_3-ZnO-Nb_2O_5 Ternary System. P J S T., vol.9
[10] Sirotinkin V.P., Bush A.A. Inorg. Mater., **39** (9) (2003) 1130-1133
[11] Kim S.S., Kim W.J. J. Cryst. Growth, **281** (2-4) (2005). 432-439
[12] Du H, Yao X. J. Phys. Chem. Solids. **63** (11) (2002) 2123-2128
[13] Nobre M.A.L., Lanfredi S. J. Mater. Sci.: Mater.Electron. **13** (4) (2002) 235-238
[14] Abrahams I, Krok F, Struzik M, Dygas J. Solid State Ionics, **179** (21-26) (2008) 1013-1017
[15] Cann D.P., Randall C.A., Shrout T.R. Solid State Commun., **100** (7) (1996) 529-534
[16] Sun D, Senz S, Hesse D. J. Eur. Ceram. Soc., **24** (8) (2004) 2453-2463
[17] Nino J.C., Lanagan M.T., and Randall C.A.. J. Appl. Phys., **89** (8) (2001) 4512–4516
[18] Wang H, Du H, Peng Z, Zhang M, Yao X. Ceram. Int., **30** (2004) 1225-1229
[19] Ren W, Trolier-Mckinstry S, Randal C.A., Shrout T.R. J. Appl. Phys. **89** (2001) 767-774